

# Use of narrowband laser speckle for MTF characterization of CCDs

*Martin Sensiper, Glenn D. Boreman, Alfred D. Ducharme, and Donald R. Snyder\**

Electrical Engineering Dept. and Center for Research in Electro-Optics and Lasers  
University of Central Florida, 12424 Research Parkway, Suite 400, Orlando, Florida 32826

\*U.S. Air Force, Wright Laboratory WL/MNGI  
Eglin Air Force Base, Florida 32542

## ABSTRACT

This paper presents a method for measuring the modulation transfer function (MTF) of a detector array from zero frequency to twice the Nyquist frequency. The equipment is simple and requires no complex optical components. Also, the use of laser speckle circumvents the problems inherent with traditional methods of MTF testing where the phase of the test target with respect to the sampling grid affects the observed contrast. The MTF measured with this method is compared to the MTF measured using sine targets. The results of the two methods agree to within 2%.

## 1. INTRODUCTION

Modulation transfer function (MTF) is recognized as the figure of merit that best describes the total spatial-frequency response of an imaging system. Widespread use of detector arrays has motivated a variety of instrumentation approaches for measuring MTF. We demonstrate a procedure that uses laser speckle to measure the response of a sampled array at any specific spatial frequency from zero frequency to twice Nyquist frequency. Ambiguities usually caused by aliasing are avoided by the use of a spatial-frequency guardband.

To date, most techniques for measuring the MTF have involved imaging bar targets, sinusoidal targets, or knife edges.<sup>1-3</sup> The use of any *imaged* target for detector-array testing is complicated by the fact that the MTF of the imaging optics must be considered. In addition, these deterministic, phase-specific scenes were originally used for deriving the spatial-frequency response of continuous-imaging systems. Detector arrays, however, have discrete elements that sample the continuous input. When this input is the image of a test target with a definite phase, the measured response is a function of the phase of the target image with respect to the structure of the sampling array.<sup>4-6</sup>

The extended knife-edge test<sup>3,7</sup> has been suggested as an approach to this phasing problem. A knife edge can be aligned precisely at an angle to the pixel columns and a superresolution scan can be created. Because the knife-edge test requires a derivative operation during the data processing, this system is particularly sensitive to noise in the high-frequency range.

Previous work<sup>8,9</sup> has demonstrated the feasibility of using laser speckle for MTF characterization. In these systems, the spatial-frequency power spectrum of the speckle is controlled by the dimensions of an aperture. The speckle is then detected on the array with no intervening optics. The power spectrum of the laser speckle has the shape of the normalized autocorrelation of the aperture intensity function, plus a delta function at zero frequency.<sup>10,11</sup> The nature of laser speckle insures that the phase of the intensity pattern is random across the detector array. Because the average power spectrum of the input is known, and the output spectrum can be measured, the transfer function can be found.

Certain assumptions must be satisfied for the above relationship between power spectrum and autocorrelation to hold. These assumptions include uniform, monochromatic coherent illumination of the aperture and linear polarization of the laser speckle. These conditions are satisfied by the design of the instrument described in Section 2. We extend the technique here by providing an appropriate method for normalization at low frequency and extend the evaluation to twice the Nyquist frequency.

## 2. INSTRUMENT DESIGN

Figure 1 shows schematically the instrument layout. This layout is similar to that proposed in Ref. 9, except for our addition of narrowband apertures. During our research, we used several laser wavelengths and tested several arrays.

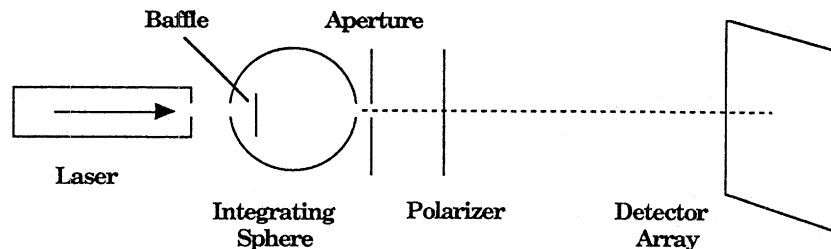


Figure 1. Optical path of test instrument.

In the visible spectrum, we used a Spectra-Physics 165 argon laser with an intracavity etalon to ensure a narrow linewidth. The wavelength was 514 nm, with an output power of 200 mW. In the near-infrared, we used a Spectra-Diode Labs SDL-5410-H1 laser diode at 848 nm with an output power of 100 mW. This laser has a linewidth of approximately 0.024 nm. The data shown in this paper are those taken using the visible laser, however the data taken using the near-infrared laser are comparable.

The Nyquist frequency,  $\xi_{\text{Nyquist}}$ , for a detector array is determined by the center-to-center separation,  $\Delta x$ , as  $\xi_{\text{Nyquist}} = 1/(2\Delta x)$ . When a discrete Fourier transform (DFT) is performed on a data set of length  $N$ , the Nyquist frequency appears at the  $N/2$  component of the DFT output. A ratio can be formed to evaluate the spatial frequency  $\xi_n$  that corresponds to the  $n^{\text{th}}$  component as

$$\frac{\xi_{\text{Nyquist}}}{N/2} = \frac{\xi_n}{n} \quad (1)$$

This associates frequencies between zero and  $\xi_{\text{Nyquist}}$  with DFT components from 0 to the  $N/2$  component. Spatial frequencies present in the continuous-input spectrum, but between Nyquist frequency and twice the Nyquist frequency, are aliased symmetrically about the Nyquist frequency into the frequency band extending from  $\xi_{\text{Nyquist}}$  back to zero. Unambiguous determination of whether the values found for the transform components pertain to aliased or unaliased frequencies depends on the input signal being bandlimited, along with the use of a spatial-frequency guardband, so that no overlap of unaliased and aliased frequencies occurs. In this case, we can unfold the aliased frequencies and plot the spatial-frequency content from zero to twice the Nyquist frequency.

When the Nyquist frequency of the array, the laser wavelength, and the dimensions of the output port of the integrating sphere are known, the aperture dimensions can be designed. The actual size and location of the features in the power spectrum (in frequency space) are scaled directly by the aperture dimensions and inversely by the wavelength and observation distance<sup>10</sup> as

$$\xi = \frac{L}{\lambda z}, \quad (2)$$

where  $\xi$  is a general spatial frequency,  $L$  is a general aperture dimension,  $\lambda$  is the laser wavelength, and  $z$  is the distance from the aperture to the observation plane.

The largest-allowed aperture dimension is determined by the size of the output port of the integrating sphere, under the consideration of uniform aperture illumination. The other dimensions of the aperture are then chosen to produce the desired power spectrum, with no overlap between unaliased and aliased frequencies, at appropriate observation distances.

A General Electric/CIDTEC TN2505 Charge Injection Device (CID) camera and an Electrim 1000 camera were both tested. The GE/CIDTEC camera has a standard RS170 analog video output and requires a Data Translation DT2851 framegrabber for data digitization. In the Electrim camera, the individual pixels are digitized with accompanying hardware. For both cameras, the data were digitized to 8 bits.

The GE/CIDTEC camera contains an anti-aliasing filter in the electronics, which attenuates the MTF to zero at the Nyquist frequency. This eliminates aliased artifacts. Because we want to demonstrate that the MTF can be measured out to twice the Nyquist frequency with laser speckle, those data are not shown here. The Electrim camera was selected for presentation of results because it contains no anti-aliasing filter and has an appreciable response at the Nyquist frequency and beyond.

For the Electrim camera, the pixel pitch in the horizontal direction is  $13.75 \mu\text{m}$ , which gives a Nyquist frequency of 36.36 cycles/mm. The detector array in this camera is 192 (horizontal) by 165 (vertical). When we transform lines of horizontal pixel data from this camera, information about the Nyquist frequency is in the 86<sup>th</sup> component. With a properly designed aperture, the output power spectrum may be measured to 72.72 cycles/mm, twice the Nyquist frequency.

The first aperture used is shown in Fig. 2. The intensity distribution,  $|P(x,y)|^2$ , in the aperture can be described as

$$|P(x,y)|^2 = \text{rect}\left(\frac{x}{l_1}\right) \text{rect}\left(\frac{y}{l_2}\right) * \left[ \left(\frac{2}{L}\right) \delta\delta\left(\frac{x}{L/2}\right) \right], \quad (3)$$

where  $*$  is the convolution operator,  $\text{rect}(x) = 1$  for  $|x| \leq 1/2$  and zero otherwise, and  $\delta\delta(x) = [\delta(x+1) + \delta(x-1)]$ , an even-impulse pair.<sup>12</sup>

Using the approach given in Section 1, the spatial-frequency power spectrum of the speckle at the observation plane,  $S(\xi,\eta)$ , is the sum of a delta function at zero frequency and the normalized autocorrelation of the aperture intensity:

$$S(\xi,\eta) = \langle I \rangle^2 \left[ \begin{aligned} &\delta(\xi,\eta) + \frac{1}{2} \frac{(\lambda z)^2}{l_1 l_2} \text{tri}\left[\frac{\xi}{l_1/\lambda z}\right] \text{tri}\left[\frac{\eta}{l_2/\lambda z}\right] \\ &+ \frac{1}{4} \frac{(\lambda z)^2}{l_1 l_2} \text{tri}\left[\frac{\xi-L/\lambda z}{l_1/\lambda z}\right] \text{tri}\left[\frac{\eta}{l_2/\lambda z}\right] \\ &+ \frac{1}{4} \frac{(\lambda z)^2}{l_1 l_2} \text{tri}\left[\frac{\xi+L/\lambda z}{l_1/\lambda z}\right] \text{tri}\left[\frac{\eta}{l_2/\lambda z}\right] \end{aligned} \right]. \quad (4)$$

In Eq. (4),  $\text{tri}(x) = 1-|x|$  for  $|x| \leq 1$  and zero elsewhere, the dimensions  $l_1$ ,  $l_2$ , and  $L$  are distances in the aperture,  $\lambda$  is the laser wavelength,  $z$  is the distance from the aperture to the observation plane, and  $\langle I \rangle^2$  is the ensemble-averaged intensity.

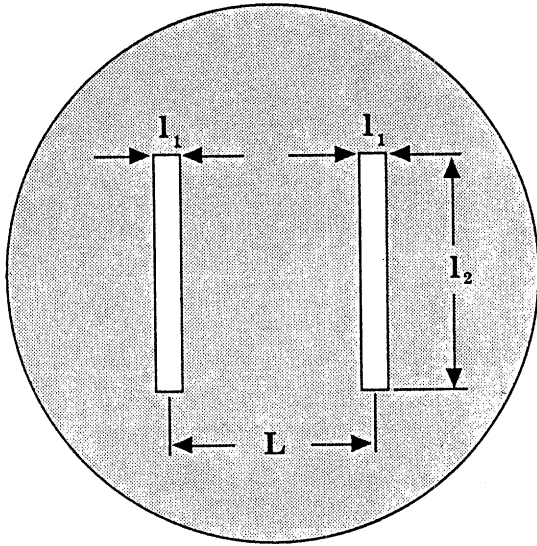


Figure 2. One-dimensional aperture.

The function in Eq. (4) is separable in  $x$  and  $y$ . Information about the power spectrum along the horizontal frequency axis of the two-dimensional transform is available as the power spectrum of the one-dimensional laser-speckle intensity taken along the horizontal spatial axis. The power spectrum in this dimension will be multiplied (and attenuated) by the horizontal MTF of the array. One-dimensional Fourier transforms can thus be performed to find the one-dimensional power spectrum,  $S(\xi)$ . Under this condition, Eq. (4) can be reduced to

$$S(\xi) = \langle I \rangle^2 \left[ \begin{aligned} &\delta(\xi) + \frac{1}{2} \frac{\lambda z}{l_1} \text{tri} \left[ \frac{\xi}{l_1/\lambda z} \right] \\ &+ \frac{1}{4} \frac{\lambda z}{l_1} \text{tri} \left[ \frac{\xi - L/\lambda z}{l_1/\lambda z} \right] \\ &+ \frac{1}{4} \frac{\lambda z}{l_1} \text{tri} \left[ \frac{\xi + L/\lambda z}{l_1/\lambda z} \right] \end{aligned} \right]. \quad (5)$$

Figure 3 shows this one-dimensional input power spectrum along the  $\xi$  direction, consisting of a baseband triangle centered at DC and two sideband triangles centered at the carrier frequency,  $\xi = \pm L/(\lambda z)$ . The features in the power spectrum scale with  $z$  as indicated by Eq. (2). As the camera is moved toward the aperture and  $z$  is decreased, the sideband triangles will move toward higher frequency and the base of all the triangles will expand. At aperture-to-camera distances in which the sideband triangles are above the Nyquist frequency, the triangles are aliased symmetrically about Nyquist into lower frequencies. Because the location and the limits of the spatial frequencies in the speckle are known, there is no ambiguity about whether or not the frequencies of interest are aliased. In our test, the high-frequency limit is set, as  $z$  is decreased, by the point at which the sideband triangles, aliased into lower and lower frequencies, begin to overlap the baseband triangle. The method by which the MTF is extracted from the raw data is described in Section 3.

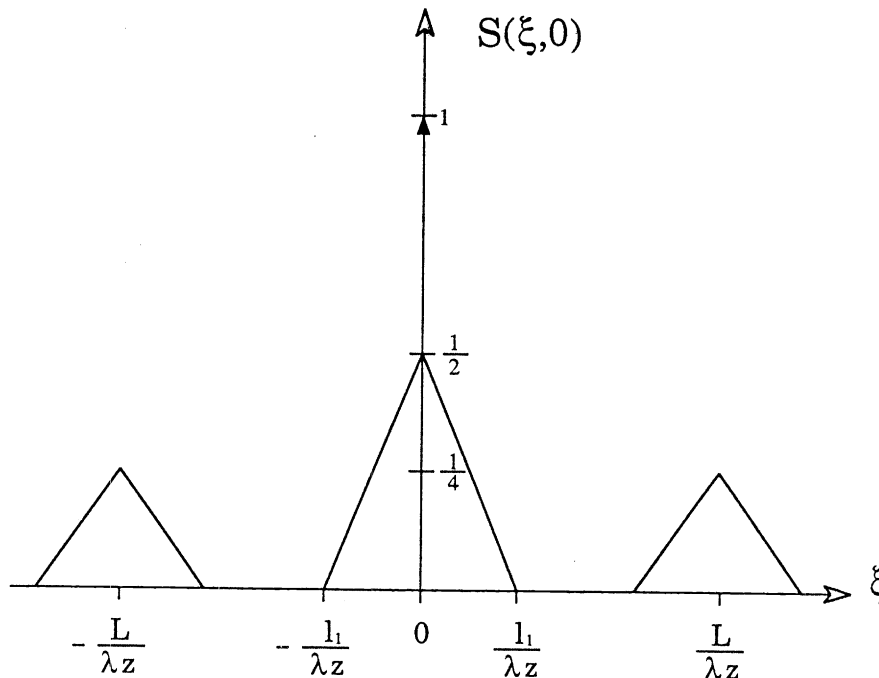


Figure 3. Power spectrum along the  $\xi$  axis with one-dimensional aperture.

### 3. DATA PROCESSING

A representative sample of the speckle detected by the array, using the aperture in Fig. 2, is shown in Fig. 4. The data exhibit both random phase and narrow spatial-frequency content. Speckle data were collected at 60 aperture-to-camera distances ranging from 45 mm to 2120 mm. Each horizontal row of data,  $s_n(x)$ , can be interpreted as a single observation of an ergodic random process. The magnitude squared of the one-dimensional Fourier transform of each row gives a single observation of the one-dimensional power spectrum,  $S_n(\xi)$ . These spectra can be ensemble averaged over the number of rows,  $n$ , to produce  $S_{ave}(\xi)$ , a more accurate estimate of the actual value of the power spectrum.

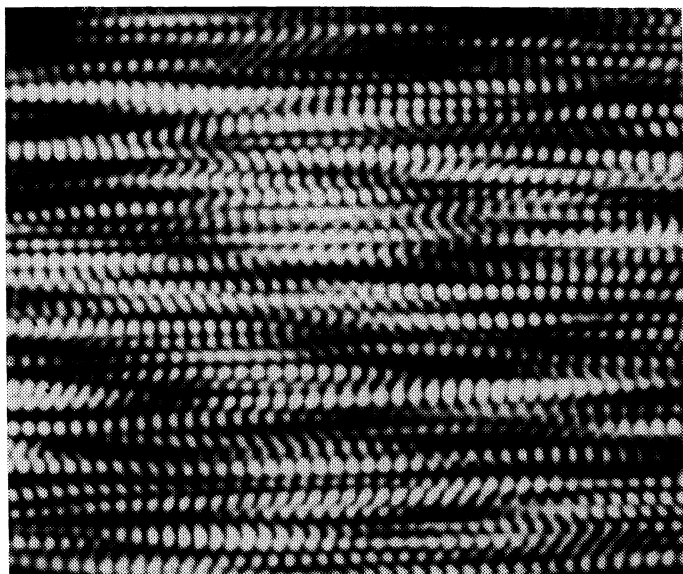


Figure 4. Sample speckle for one-dimensional data.

Figure 3 and Eq. (5) illustrate several important features in the input power spectrum. First, the baseband triangle centered at zero frequency has twice the amplitude of the sideband triangles. The height of the sideband triangles will be attenuated by the array MTF at the frequency where they are located. The baseband triangle peak can be normalized to 1. We can determine the amount of attenuation by comparing the unattenuated peak of the baseband triangle with the peak of the sideband triangles. However, the value at the peak of the baseband triangle is masked by the delta function at DC seen in Eq. (5). If we can excise this delta function, while leaving the DC value of the baseband triangle intact, the MTF can be correctly normalized.

We excise the delta function by inverse Fourier transforming the average power spectrum,  $S_{ave}(\xi)$ , and obtaining an average autocorrelation,  $R_{ave}(x)$ . In this domain the zero frequency delta function is now a constant offset and is the minimum value of  $R_{ave}(x)$ . We subtract this minimum value and obtain a normalized autocorrelation,  $R_{norm}(x)$ . This function is then retransformed to produce the power spectrum,  $S_{norm}(\xi)$ , which is normalized to 1 at zero frequency.

We plot two representative profiles of the normalized one-dimensional output power spectrum,  $S_{out}(\xi)$ , in Fig. 5. The unaliased positive spatial frequencies (solid line) are noted along the horizontal axis from zero to the Nyquist frequency, and the aliased frequencies (dotted line) are noted, below their low frequency aliases, from the Nyquist frequency to twice the Nyquist frequency. Because we know all the factors on the right side of Eq. (2) for each image, there is no doubt about whether or not the triangle is aliased. The data can be read off the appropriate scale and unfolded to form a response curve from zero to twice Nyquist. The MTF calculated from these data is shown in Section 5.

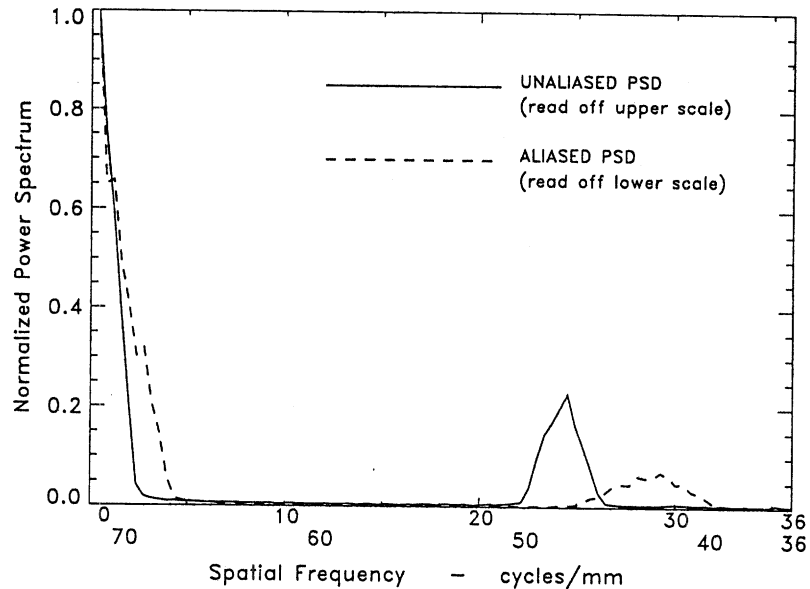


Figure 5. Examples of unaliased and aliased power spectra.

The MTF is the magnitude of the optical-system transfer function. As developed in linear-systems theory, the relationship between input power spectral density,  $S_{in}(\xi)$ , output power spectral density,  $S_{out}(\xi)$ , and the magnitude of the system transfer function,  $H(\xi)$ , are related by

$$S_{out}(\xi) = |H(\xi)|^2 S_{in}(\xi) . \quad (6)$$

We can find one point on the MTF curve at the frequency  $\xi_{peak}$  by using this equation and knowing that in the normalized input, the peak of the modulated triangle,  $S_{in}(\xi_{peak})$ , has a value of one-half.

During collection of the data, the approximate aperture-to-camera distance was recorded. A precise measurement of this distance is extremely difficult because of the camera housing, the small distances involved, and the close quarters of the components. However, this does not present a problem in the data interpretation. Deviations from the measured distance or a slight tilt in the aperture-to-pixel column alignment can shift the triangle peak. The approximate distance and Eqs. (1) and (2) are used to search for the peak as a local maximum in the transform components. Because each component can be associated with a specific spatial frequency, we can determine the exact spatial frequency at which the peak occurs. That means the procedure is essentially self calibrating, a distinct advantage over other methods.

## 5. MTF RESULTS

The MTF in the horizontal direction for the Electrim 1000 camera is presented in Fig. 6 (solid line). As described in Section 1, this MTF is for the array only. The data points are shown along with a third-order polynomial fitted to the points.

To compare our array MTF results with results from sine-wave testing, we obtained the MTF for the imaging lens using an Ealing Eros MTF Analyzer. The lens and the camera were then used to measure the system response by imaging precision sinusoidal test targets from a commercial transparency.<sup>13</sup> The MTF at each sinusoidal frequency was calculated as

$$MTF(\xi) = \frac{\text{pixel}_{\max} - \text{pixel}_{\min}}{\text{pixel}_{\max} + \text{pixel}_{\min}}, \quad (7)$$

where  $\text{pixel}_{\max}$  and  $\text{pixel}_{\min}$  are adjacent maximum and minimum values in the sine-wave data.

The array MTF and lens MTF, measured separately then multiplied together, should equal the system MTF measured by imaging the sinusoids. This comparison is seen in Fig. 6. The speckle MTF method produces useful data over a wider frequency range because of noise limitations in the sine-wave method. The curves agree to within 2%.

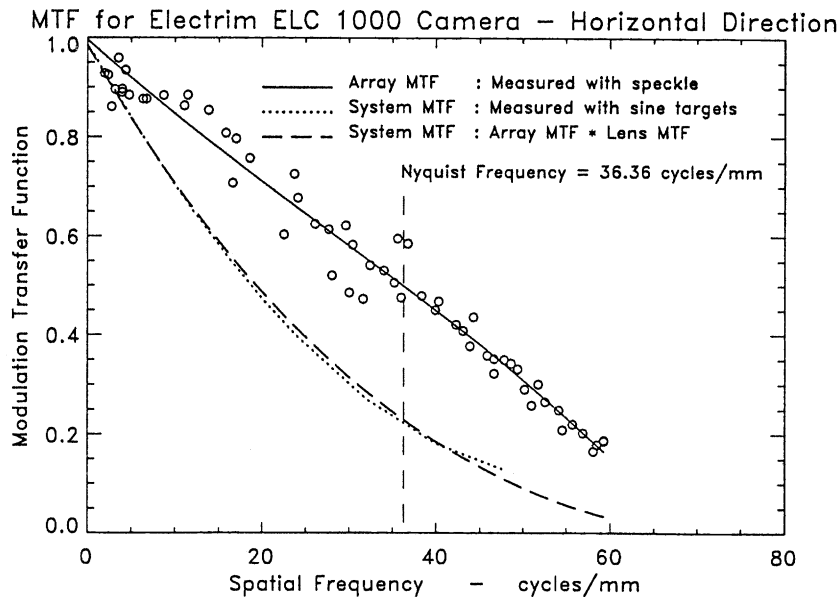


Figure 6. MTF of Electrim camera array using laser speckle and system MTF with sine targets vs system MTF as an array MTF times lens MTF.

## 6. CONCLUSIONS

We have demonstrated the use of laser speckle for measuring the MTF of detector arrays from DC to twice the Nyquist frequency. Our results compare well with those from a standard sine-wave measurement. Agreement was found to be within 2%. The availability and ease of fabrication of the components, plus the ability to set up a test bed with minimal calibration, make the method a potential solution to practical MTF testing of arrays. The method is essentially self calibrating, in that the modulation depth and the spatial frequency for any data point are both measured values. Because the optical path contains no imaging optics, the method measures the MTF of the array directly. In addition, this method is applicable over a wide range of wavelengths.

## 7. ACKNOWLEDGMENTS

This work was supported by the U.S. Air Force, Wright Laboratory, under contract DAA-B07-88-C-F-405-ARPA-6324.

## REFERENCES

1. S. B. Campana, "Techniques for Evaluating Charge Coupled Imagers," *Opt. Eng.* 16(3), 2267-2274 (1977).
2. S. K. Park, R. Schowengerdt, and M. Kaczynski, "Modulation-Transfer-Function Analysis for Sampled Image Systems," *Appl. Opt.* 23(15), 2572-2582 (1984).
3. S. E. Reichenbach, S. K. Park, and R. Narayanswamy, "Characterizing Digital Image Acquisition Devices," *Opt. Eng.* 30(2), 170-177 (1991).
4. W. Wittenstein et al., "The definition of the OTF and the Measurement of Aliasing for Sampled Imaging Systems," *Opt. Acta* 29(1), 41-50 (1982).
5. R. Legault, in *Perception of Displayed Information*, L. M. Biberman, ed., pp. 279-312, Plenum, New York (1973).
6. J. Feltz and M. Karim, "Modulation Transfer Function of Charge-Coupled Devices," *Appl. Opt.* 29(5), 717-722 (1990).
7. H. Wong, "Effect of Knife-Edge Skew on Modulation Transfer Function Measurements of Charge-Coupled Device Imagers Employing a Scanning Knife Edge," *Opt. Eng.* 30(9), 1394-1398 (1991).
8. G. Boreman, Y. Sun, and A. James, "Generation of Laser Speckle with an Integrating Sphere," *Opt. Eng.* 29(4), 339-342 (1990).
9. G. Boreman and E. Dereniak, "Method for Measuring Modulation Transfer Function of Charge-Coupled Devices using Laser Speckle," *Opt. Eng.* 24(1), 148-150 (1986).
10. J. Goodman, in *Laser Speckle and Related Phenomena*, J. C. Dainty, ed., pp. 35-40, Springer-Verlag, Berlin (1975).
11. L. Goldfischer, "Autocorrelation Function and Power Spectral Density of Laser-Produced Speckle Patterns," *J. Opt. Soc. Am.* 55(3), 247-253 (1965).
12. J. Gaskill, *Linear Systems, Fourier Transforms, and Optics*, p. 57, Wiley, New York (1978).
13. Sine Patterns Catalog, Sine Patterns Inc., Penfield, N.Y. (1990).